AD-A043 522 BENDIX CORP TETERBORO N J FLIGHT SYSTEMS DIV F/G 1/2
IMPROVED FLARE LAW STUDY.(U)
DEC 74 V MUEHTER

UNCLASSIFIED AFFDL-TR-77-71 F33615-72-C-1753 NL

| OF |
AD A043522

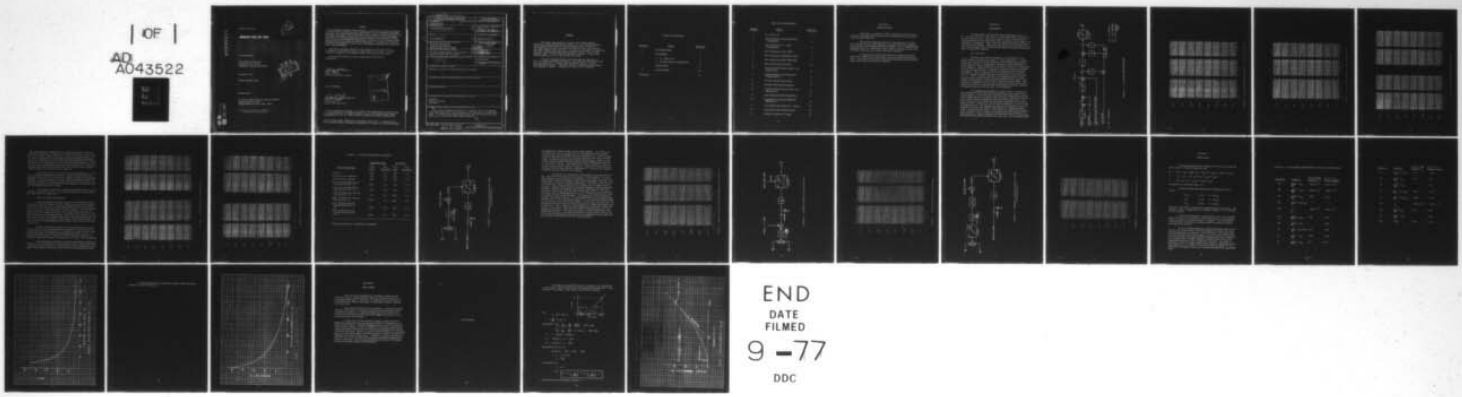

END
DATE FILMED
9 -77
DDC

AFFDL-TR-77-71

12

IMPROVED FLARE LAW STUDY

Vincent Muehter

The Bendix Corporation
Flight Systems Division
Teterboro, New Jersey 07608

December 1974

FINAL REPORT A006

Prepared for:

Air Force Flight Dynamics Laboratory/FGT
United States Air Force
Wright-Patterson AFB, Ohio 45433

APPROVED FOR PUBLIC RELEASE;
DISTRIBUTION UNLIMITED

NOTICE

When Government drawings, specifications, or other data are used for any purpose other than in connection with a definitely related Government procurement operation, the United States Government thereby incurs no responsibility nor any obligation whatsoever; and the fact that the government may have formulated, furnished, or in any way supplied the said drawings, specifications, or other data, is not to be regarded by implication or otherwise as in any manner licensing the holder or any other person or corporation, or conveying any rights or permission to manufacture, use, or sell any patented invention that may in any way be related thereto.

This report has been reviewed by the Information Office (OI) and is releasable to the National Technical Information Service (NTIS). At NTIS it will be available to the general public, including foreign nations.

This technical report has been reviewed and is approved for publication.

Jim J. Guckian

JIM J. GUCKIAN
Project Engineer
Terminal Area Control Branch

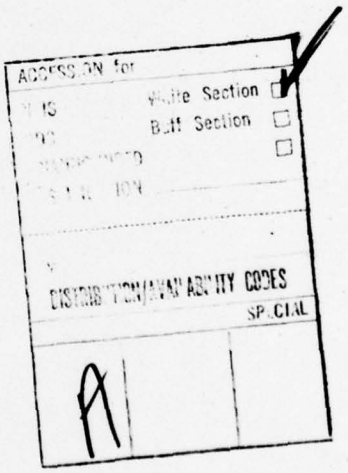

FOR THE COMMANDER

Robert P. Johannes

ROBERT P. JOHANNES
Acting Chief
Flight Control Division

"If your address has changed, if you wish to be removed from our mailing list, or if the addressee is no longer employed by your organization please notify AFFDL/STINFO ,W-P AFB, OH 45433 to help us maintain a current mailing list".

Copies of this report should not be returned unless return is required by security considerations, contractual obligations, or notice on a specific document.

UNCLASSIFIED

SECURITY CLASSIFICATION OF THIS PAGE (When Data Entered)

REPORT DOCUMENTATION PAGE

READ INSTRUCTIONS BEFORE COMPLETING FORM

1. REPORT NUMBER: AFFDL-TR-77-71	2. GOVT ACCESSION NO.
3. RECIPIENT'S CATALOG NUMBER	
4. TITLE (and Subtitle): IMPROVED FLARE LAW STUDY.	5. TYPE OF REPORT & PERIOD COVERED: Final rept. Jan 1972 - Dec 1974
6. PERFORMING ORG. REPORT NUMBER	
7. AUTHOR(s): Vincent Muehter	8. CONTRACT OR GRANT NUMBER(s): F33615-72-C-1753
9. PERFORMING ORGANIZATION NAME AND ADDRESS: The Bendix Corporation, Flight Systems Division, Teterboro, New Jersey 07608	10. PROGRAM ELEMENT, PROJECT, TASK AREA & WORK UNIT NUMBERS: 62201F 82260121 01
11. CONTROLLING OFFICE NAME AND ADDRESS: Air Force Flight Dynamics Laboratory/FGT, Wright-Patterson AFB, OH 45433	12. REPORT DATE: December 1974
	13. NUMBER OF PAGES: 31
14. MONITORING AGENCY NAME & ADDRESS (if different from Controlling Office) 33p.	15. SECURITY CLASS. (of this report): Unclassified
	15a. DECLASSIFICATION/DOWNGRADING SCHEDULE

16. DISTRIBUTION STATEMENT (of this Report)

Approved for public release; distribution unlimited

17. DISTRIBUTION STATEMENT (of the abstract entered in Block 20, if different from Report)

18. SUPPLEMENTARY NOTES

19. KEY WORDS (Continue on reverse side if necessary and identify by block number)

Automatic
Aircraft Landings
Wind Shear

20. ABSTRACT (Continue on reverse side if necessary and identify by block number)

This report contains the results of a computer study on an improved flight path angle flare law using altitude and range data as command parameters. Throttle retard compensation during flare was considered for the head, tail, no wind, and various shear conditions.

DD FORM 1 JAN 73 1473 EDITION OF 1 NOV 65 IS OBSOLETE

409 146

UNCLASSIFIED

SECURITY CLASSIFICATION OF THIS PAGE (When Data Entered)

FOREWORD

This report was prepared for the Air Force Flight Dynamics Laboratory, Flight Research and Test Branch, Air Force Systems Command, by the Flight Systems Division, The Bendix Corporation, Teterboro, New Jersey under Air Force Contract No. F33615-72-C-1753, data document item A006, Improved Flare Law Study. This work was performed in conjunction with other program tasks during the time period January, 1972, through December, 1974. The Air Force Program Manager was Capt T. Imrich with Project Engineers, Lt R. P. Denaro and Lt B. Kunciw.

The Flight Systems Division effort was under the direction of Mr. F. G. Adams, principal investigator. The simulation and analysis task was conducted by Mr. V. Muehter with contributions by Mr. K. Moses, Assistant Chief Engineer. Supporting data and configuration requirements were supplied by Messrs. J. Woloshen, M. Sforza, and S. Skaritka.

TABLE OF CONTENTS

LIST OF ILLUSTRATIONS

SECTION 1

INTRODUCTION

This study, in response to data document item A006 was performed to investigate improved control law concepts in the flare portion of the automatic approach.

The present exponential flare law, using altitude (h) and derived altitude rate ($\dot{h}$) yields satisfactory results under most conditions. It was felt that in using information now available, such as range (R) and flight path angle (γ), reductions could be made in touchdown dispersions presently occurring under certain wind shear conditions.

A study was also performed in the area of advanced throttle control as a modification to the present open loop throttle retard during flare. This effort was directed toward optimizing airspeed bleeds during flares under varying wind shear conditions.

SECTION 2

DISCUSSION

The present KC-135 automatic flare configuration uses, $h + \tau\dot{h} = 0$ as its control law. This forces an exponential altitude characteristic with respect to time. It is noted, however, that no restoring term exists should the aircraft deviate from the nominal flare path in space, due to gusting or windshears. The control law merely requires a particular sink rate at each altitude. Thus consistent sink rates at touchdown are its main characteristic with a considerable sacrifice in touchdown dispersions under varying wind conditions.

1. R, γ Flare Law

The flare law herein investigated, as an alternative to the present system, is depicted in Figure 1. This is basically a γ control system which indirectly controls sink rate at touchdown with small variations from nominal, corresponding to changes in ground speed due to wind conditions. These variations, in the order of 14% for a 20 knot wind, are considered a small price to pay for a system which does not deviate from the nominal flare path to maintain a particular sink rate during wind shears. The γ command term can be considered to be a direct function of altitude when the aircraft is tracking the nominal flare path ($h_\epsilon = 0$). The h command term ($\hat{h}$) is a computed function of range (referenced to a point on runway 1000 feet behind the glide slope transmitter) corresponding to the nominal no wind flare path in space. This additional computed h error (h_ϵ) term prevents the system from allowing the aircraft to fly a path parallel to the nominal flare path, should it be displaced therefrom for any reason (see Appendix).

To investigate the feasibility of such a system, comparisons were made between it and the present exponential system under various wind conditions. The wind models used were those suggested by the Air Force Flight Dynamics Laboratory and consisted of constant head and tail winds, linear shears, logarithmic shears and knife-edge shears. The flare responses for the nominal and proposed configuration are shown in Figures 2 and 3, respectively, for the 20 knot headwind, no wind, and 20 knot tailwind cases. As expected, the sink rate at touchdown for the exponential flare was held constant at the expense of longitudinal dispersions. The proposed R, γ flare, on the other hand, allowed approximately a 15% variation from its nominal (no wind) sink rate but displayed very little dispersion. Figure 4 displays the flare performance in 20 knot head and tail winds sheared out linearly from 500-0 feet. It is noted that the R,

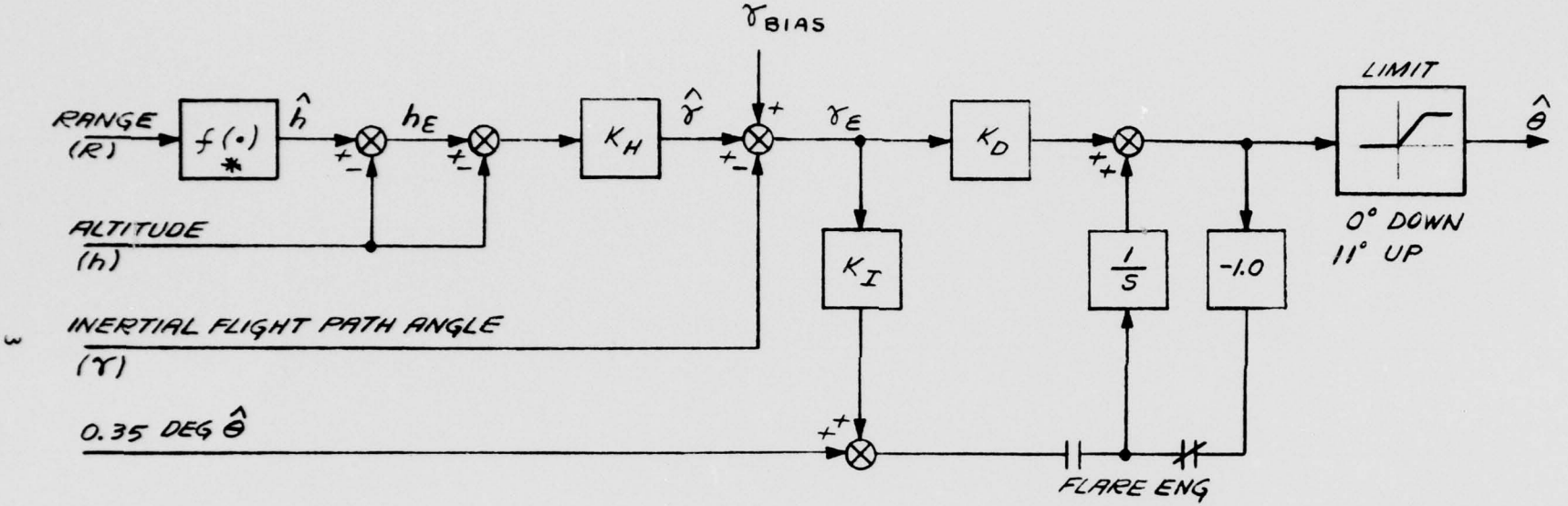

FIGURE 1. R, γ FLARE CONFIGURATION

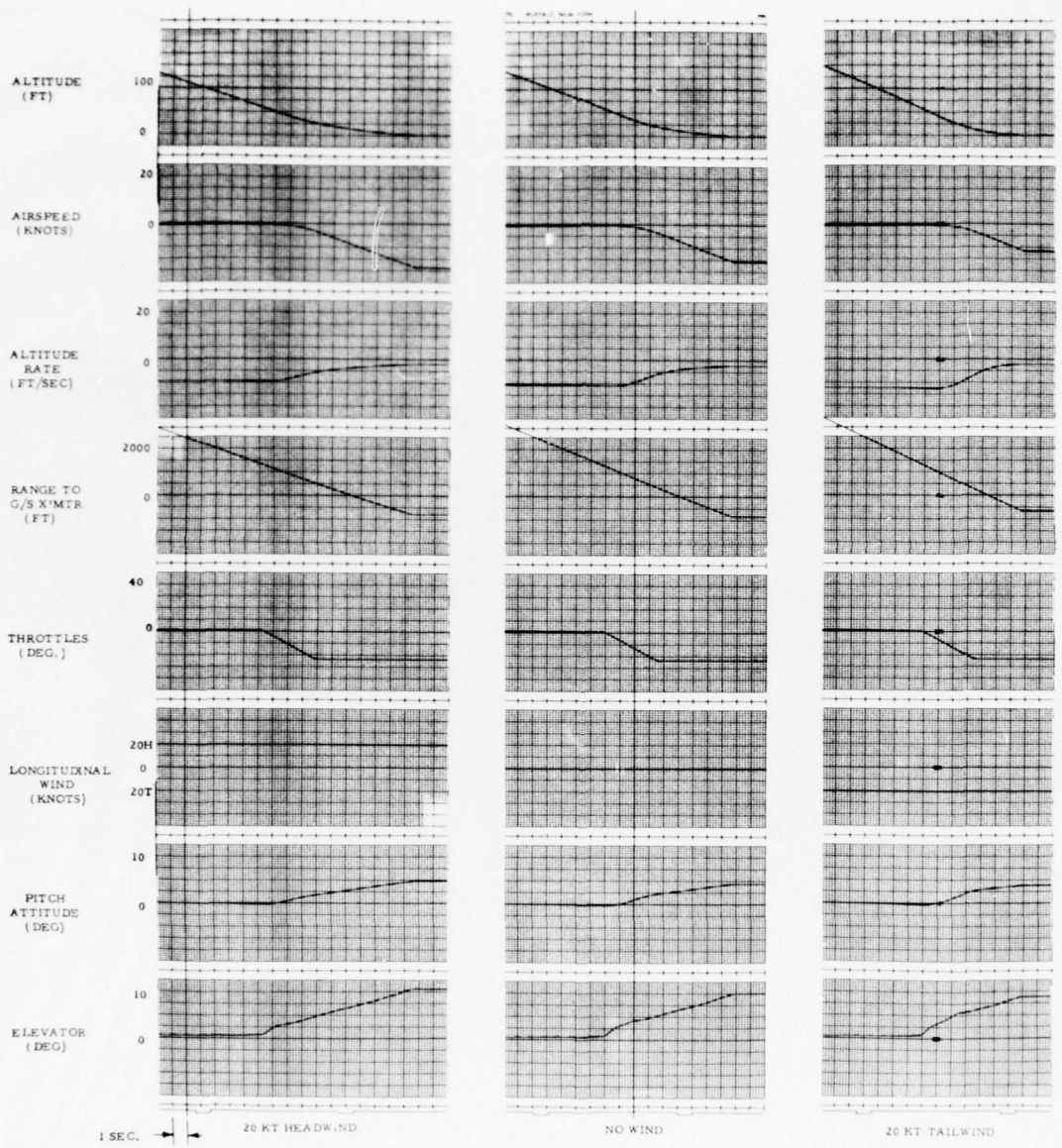

FIGURE 2. FLARE RESPONSES-EXPONENTIAL FLARE CONFIGURATION

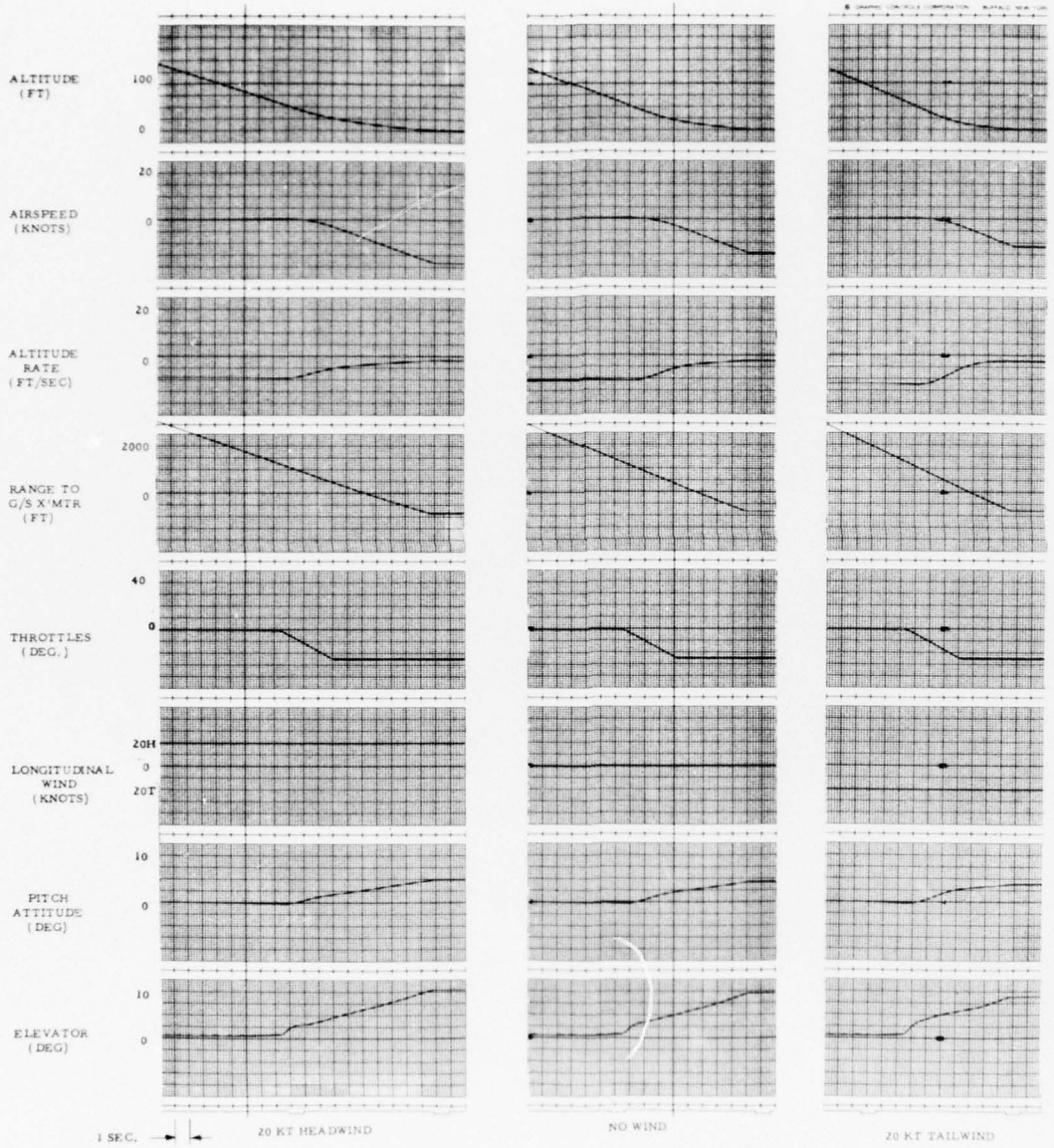

FIGURE 3. FLARE RESPONSES-R, Υ FLARE CONFIGURATION

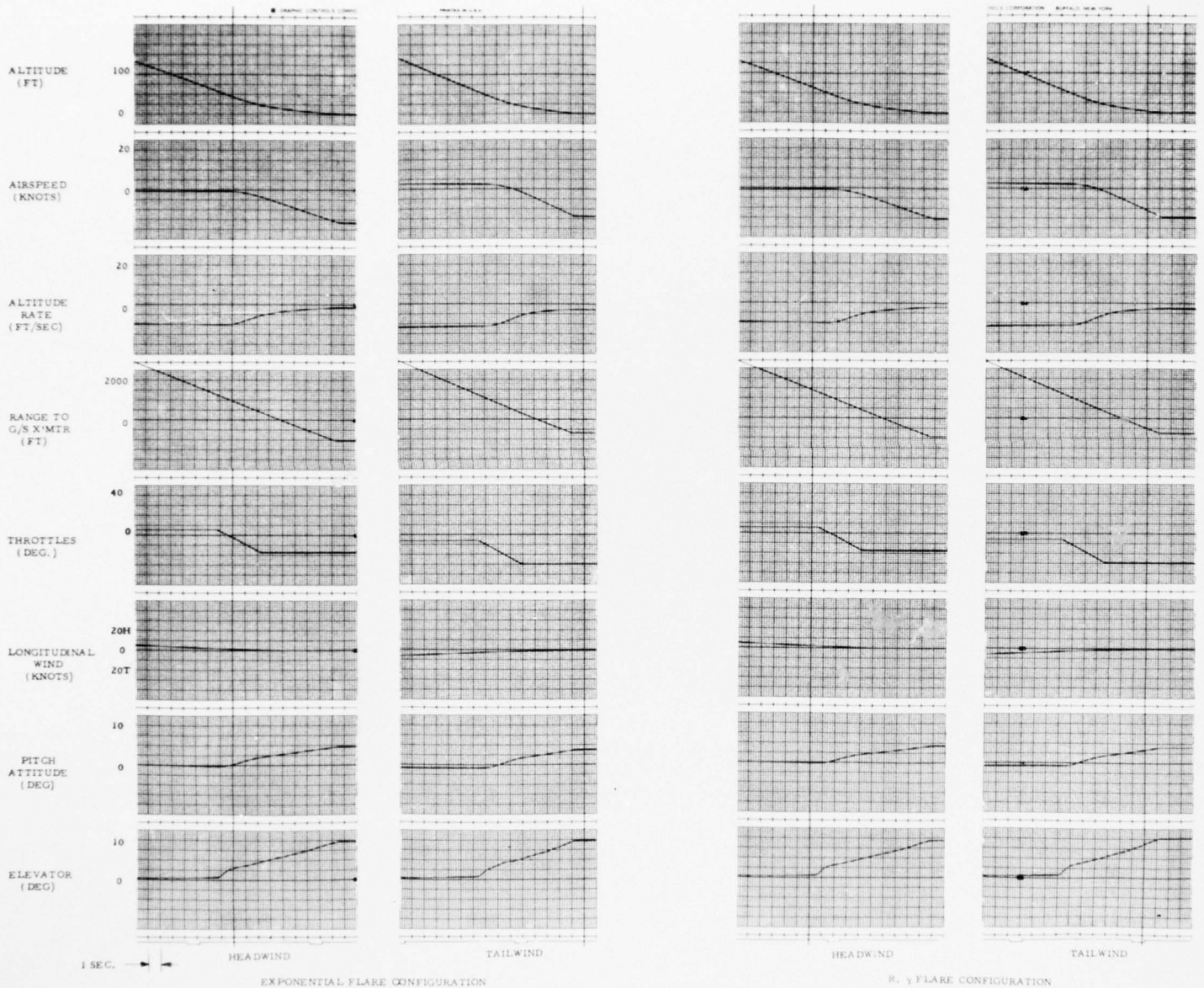

FIGURE 4. FLARE RESPONSES-LINEAR SHEAR

γ flare has displayed considerably less touchdown dispersion and at the same time resulted in less variation in touchdown sink rate. It was found that in cases where winds were sheared to near zero at ground level, the R, γ flare configuration not only yielded smaller longitudinal dispersions but also less variations in sink rate than the exponential system. The latter is due to the combination of the aircraft's increased ability to remain on the nominal γ path and the absence of wind at ground level. These same characteristics are demonstrated for the case of 20 knot winds logarithmically sheared out from 500-0 feet in Figure 5.

Knife-edge shears at 110 feet from 20 knots shearing to 13 knots were simulated during flares in Figure 6. Again touchdown dispersion characteristics for the R, γ flare are far superior to those of the exponential flare. This type of shear was found to cause the greatest variation in touchdown sink rate for the R, γ system. Even in this case, however, the choice to accept a somewhat larger sink rate variation to ensure far smaller longitudinal dispersions is clear.

The results of all the above referenced simulated flares are summarized in the table of Figure 7. The overall superiority of the proposed R, γ flare system is quite evident.

2. Throttle Retard Considerations

In the present KC-135 throttle system, the autothrottle output is frozen at zero at the initiation of flare. At this time an open loop ramp is fed to the throttle servo as a constant rate throttle retard, up to a fixed limit. The rate and limit have been chosen to provide an optimum airspeed bleed during flare, under the nominal, no wind condition. An optimum bleed in this case is approximately 15 knots, which would still allow a sufficient margin above the stall airspeed. Referring back to Figure 2, it has been shown that for 20 knot head and tail winds, the airspeed bleed can vary from 19 to 12 knots respectively. This is due to the fact that the time for flare is larger in a headwind than tailwind and the rate of bleed is the same in each case.

These airspeed bleed variations would suggest the use of some form of closed loop around the throttles based upon a comparison between ground speed (Vg) and airspeed (Va). Studies have shown, however, that the slow response of airspeed to throttle position precludes the use of a closed loop linear system. Therefore, various non-linear schemes, in which the retard rate and limit are functions of (Va-Vg), were investigated.

One configuration intended to minimize the airspeed variations of Figure 2, is shown in Figure 8. The presence of either a head or tail wind is sensed by comparing Vg with Va and the retard limit is adjusted accordingly. The results of the present system flares incorporating this feature

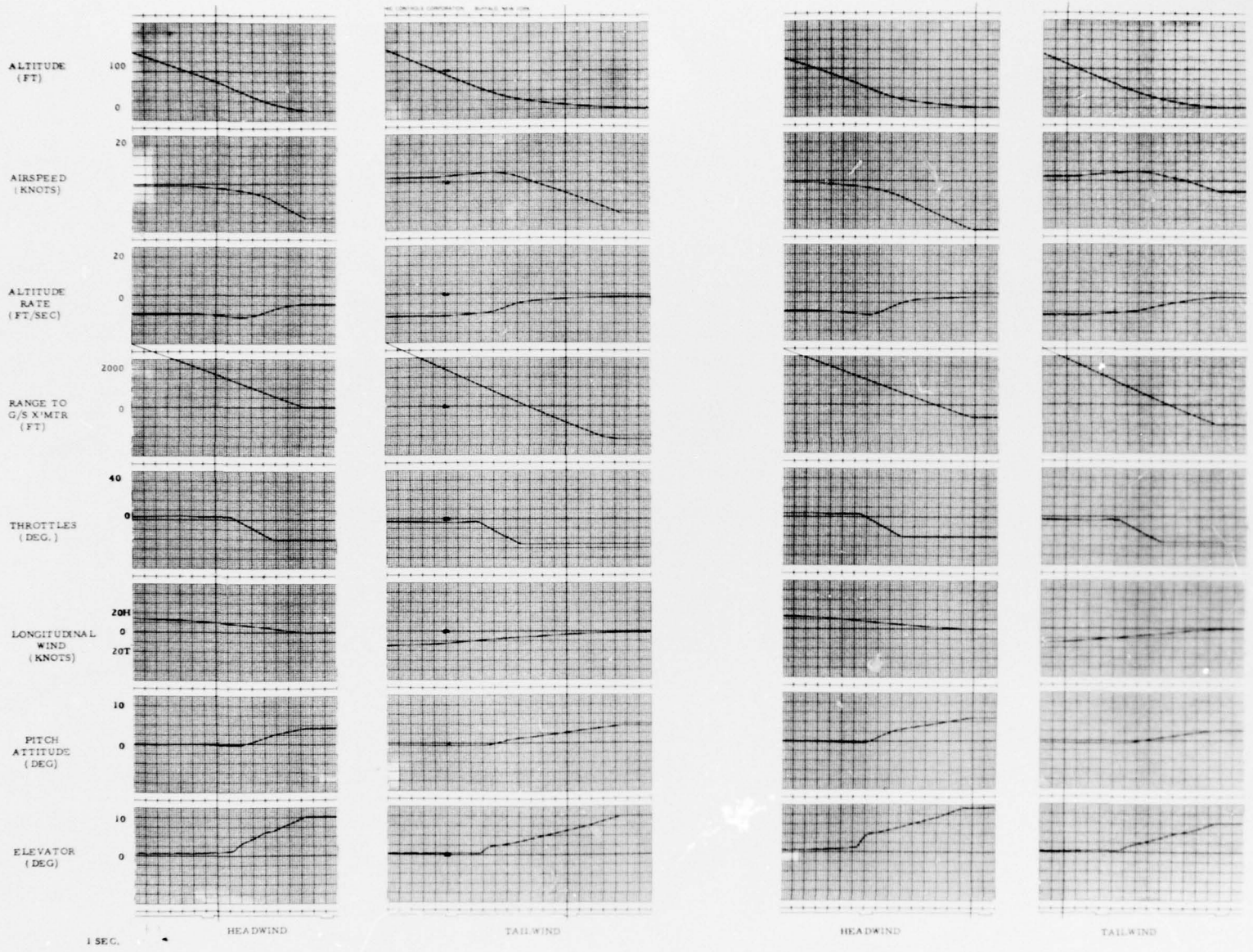

FIGURE 5. FLARE RESPONSES-LOGARITHMIC SHEAR

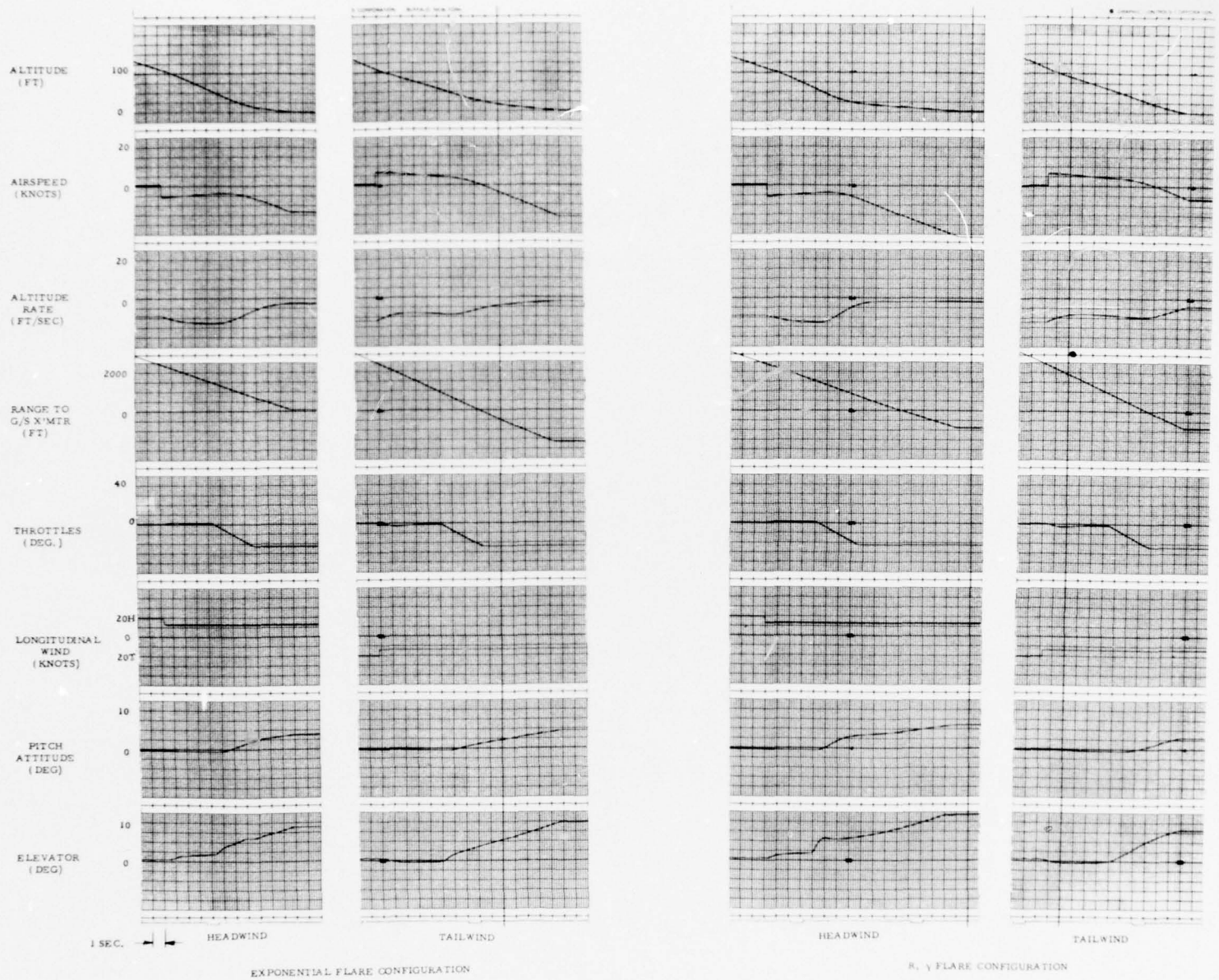

FIGURE 6. FLARE RESPONSES-KNIFE-EDGE SHEAR

FIGURE 7. FLARE PERFORMANCE SUMMARY

WIND CONDITIONS	Exponential Flare		R, γ Flare	
	X_{TD}* (Ft.)	$\dot{h}_{TD}$ (Ft./Sec.)	X_{TD}* (Ft.)	$\dot{h}_{TD}$ (Ft./Sec.)
No Wind	-810	-2.0	-800	-2.2
Constant 20 Kt. Headwind	-800	-2.0	-850	-1.9
Constant 20 Kt. Tailwind	-650	-2.0	-800	-2.5
20 Kt. Headwind Sheared Out Linearly from 500' - 0'	+1030	-1.5	-900	-2.0
20 Kt. Tailwind Sheared Out Linearly from 500' - 0'	-680	-2.8	-730	-2.5
20 Kt. Headwind Log. Sheared Out from 500' - 0'	+30	-4.2	-640	-2.0
20 Kt. Tailwind Log. Sheared Out from 500' - 0'	-1700	-1.5	-1000	-2.2
20 Kt. Headwind and 7 Kt. Knifedge Sheared Out at 110'	+100	-2.4	-860	-1.8
20 Kt. Tailwind and 7 Kt. Knifedge Sheared Out at 110'	-1650	-2.0	-830	-4.0

*Distance Referenced to Glide Slope Transmitter

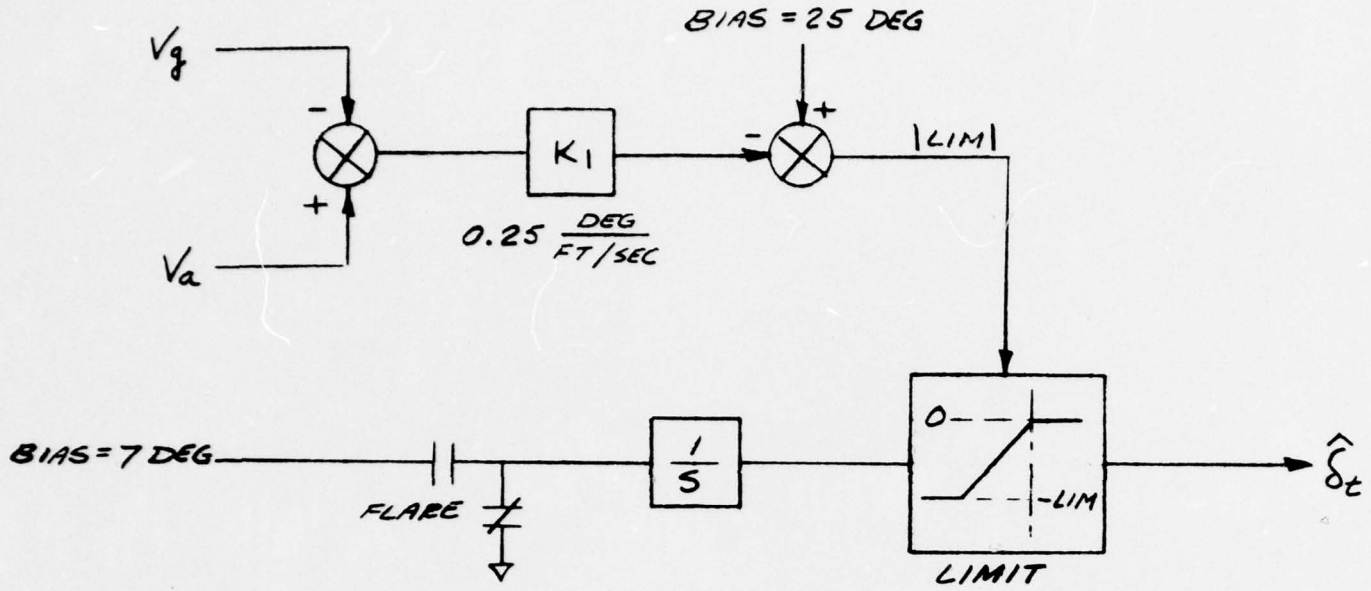

FIGURE 8. VARIABLE THROTTLE RETARD LIMIT
CONFIGURATION #1

are displayed in Figure 9 under various wind conditions. It is noted, the characteristic of more airspeed bleed in a headwind has still remained despite the fact that the throttles have not retarded as far. This is caused by the fact that the time for flare has been affected by the level of throttle retard, through the pitching moment due to thrust ($M_{\Delta T}$). Figure 10 describes another method controlling throttle retard by adjusting retard rate as a function of (Va-Vg). Its responses are shown in Figure 11 and show similar characteristics to those of Figure 9. Therefore, it seems that any attempt to alter airspeed bleed to compensate for a constant wind condition, by altering throttle retard is self defeating.

Compensation for wind shears, during flares, may still be possible. This has been an area of prime concern. The occurrence of a knife-edge shearing out of a headwind or shearing in of a tailwind may reduce airspeed close to stall levels using an open loop throttle retard. Therefore, the configuration of Figure 12 has been under study. The object of this scheme is to reduce the nominal retard limit as a function of only sudden drops in airspeed. These would be caused by airspeed changes too rapid to allow the aircraft to maintain its airspeed, thus the use of the washout. Therefore, the time of flare would not be affected, as discussed above, unless a serious wind shear such as a knife-edge were to occur. In that event the limit would be reduced to help maintain airspeed. The responses of this configuration and that of the present system, to 20 knots headwind with 10 knots knife-edge sheared out at 30 feet, are shown in Figure 13. It is noted that improvements can be seen due to the reduced retard limit. As the shear is encountered, the retarded throttles are driven back toward positive to oppose the instantaneous airspeed loss. This results in a total airspeed loss comparable to that of the nominal no wind flare. Sink rate and touchdown dispersion have also been significantly improved. This shear occurred at a point approximately mid-point during the flare. It is noted that shears occurring closer to the ground could not be compensated for as well since the resulting forward throttle motion would have less time to effect the overall problem.

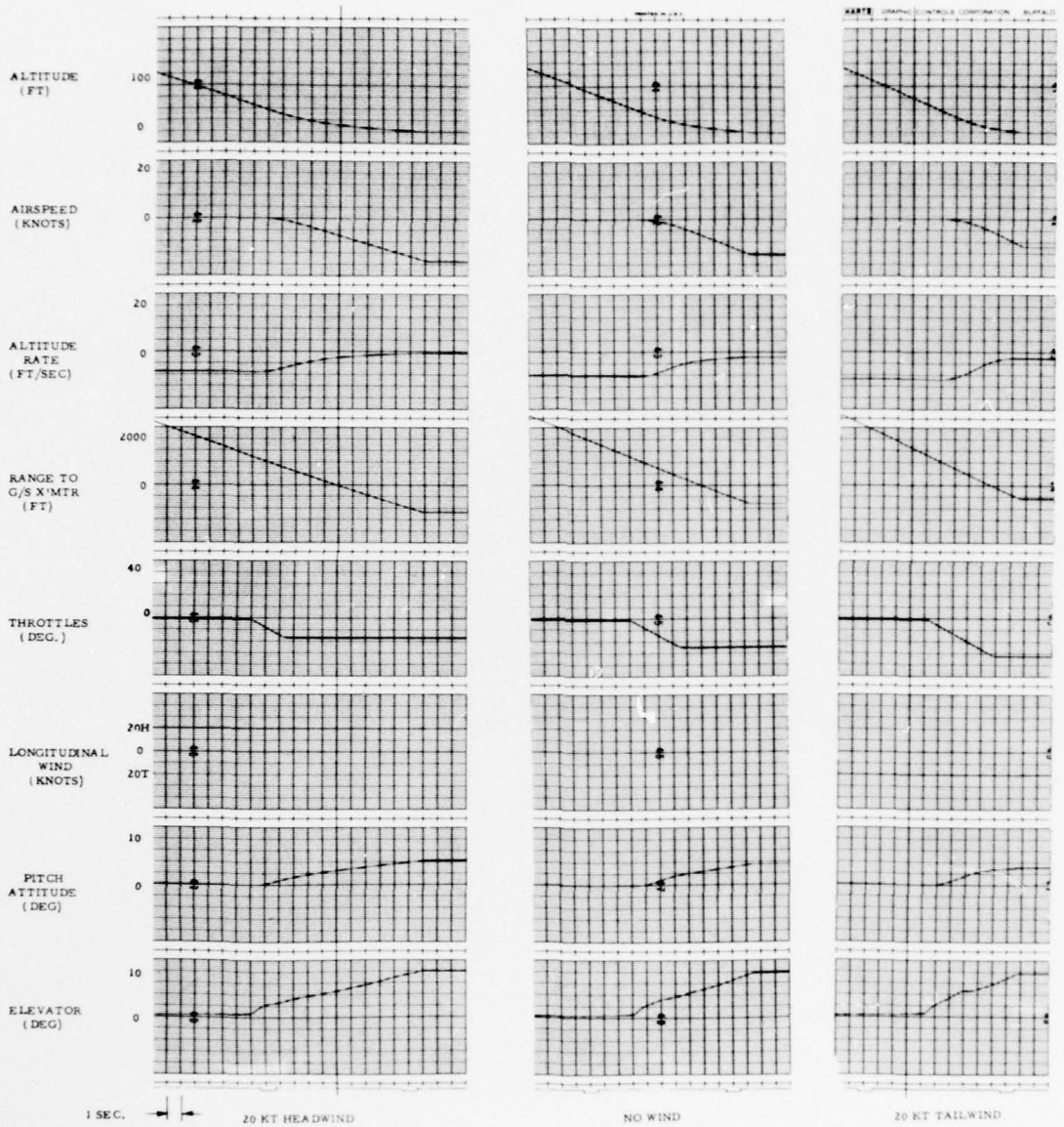

FIGURE 9. VARIABLE RETARD LIMIT RESPONSES-CONFIGURATION #1

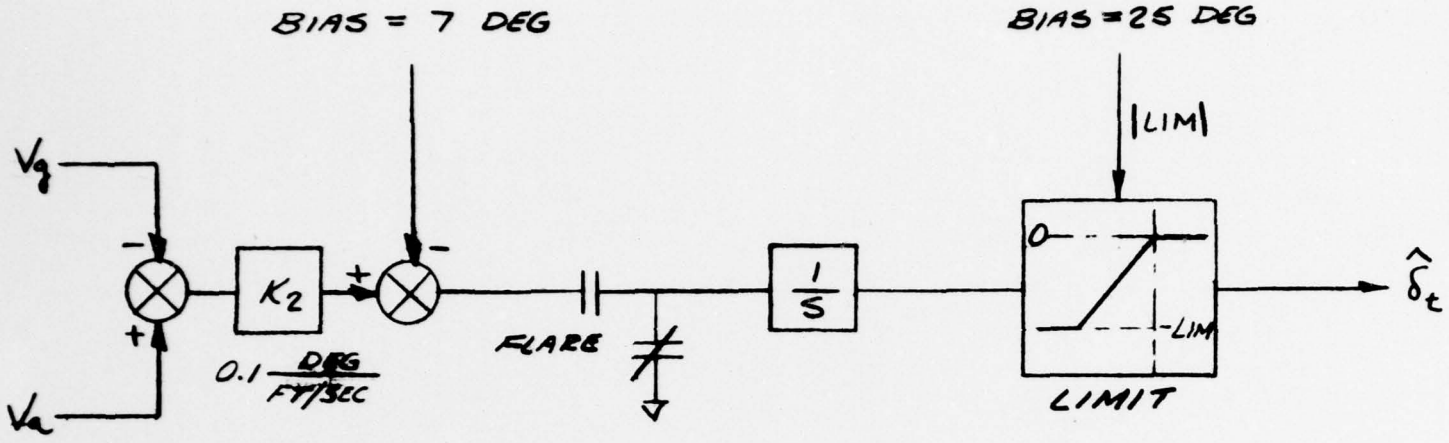

FIGURE 10. VARIABLE THROTTLE RETARD RATE

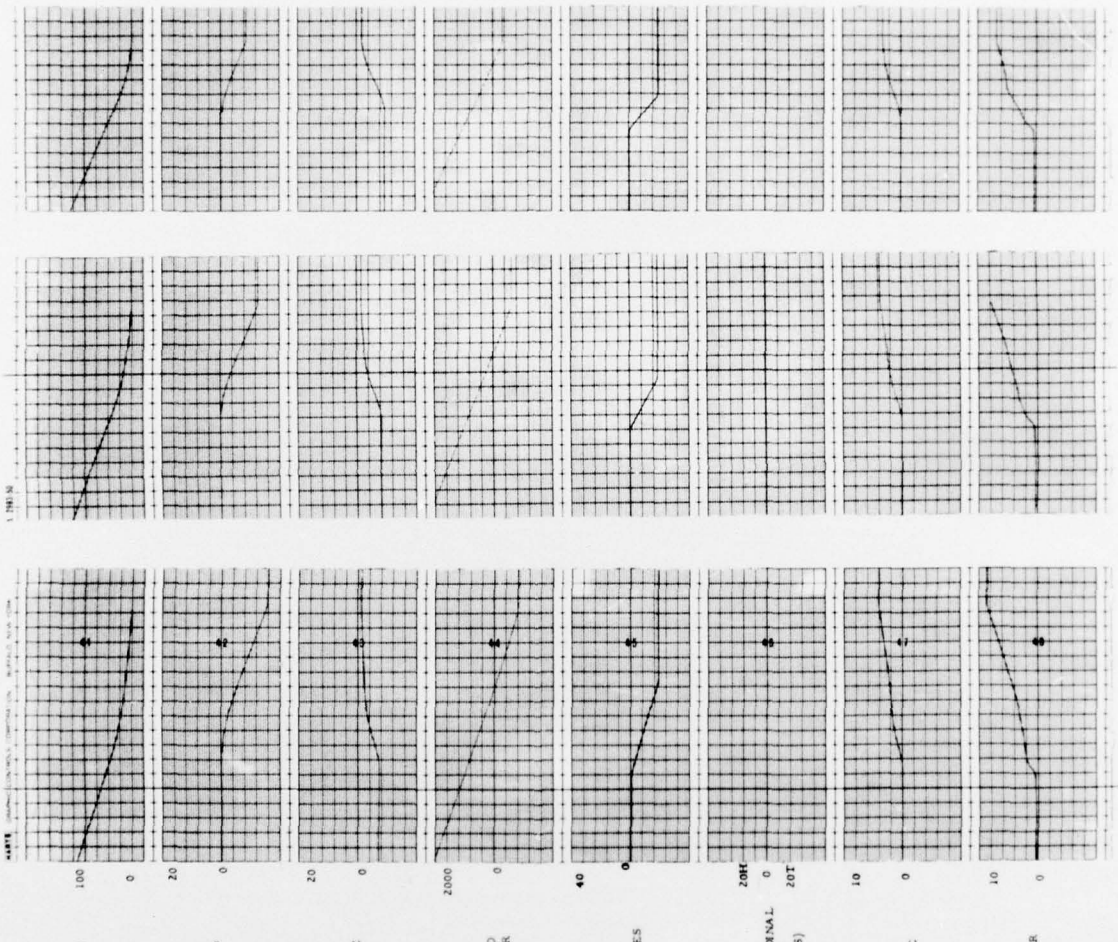

FIGURE 11. VARIABLE RETARD RATE RESPONSES

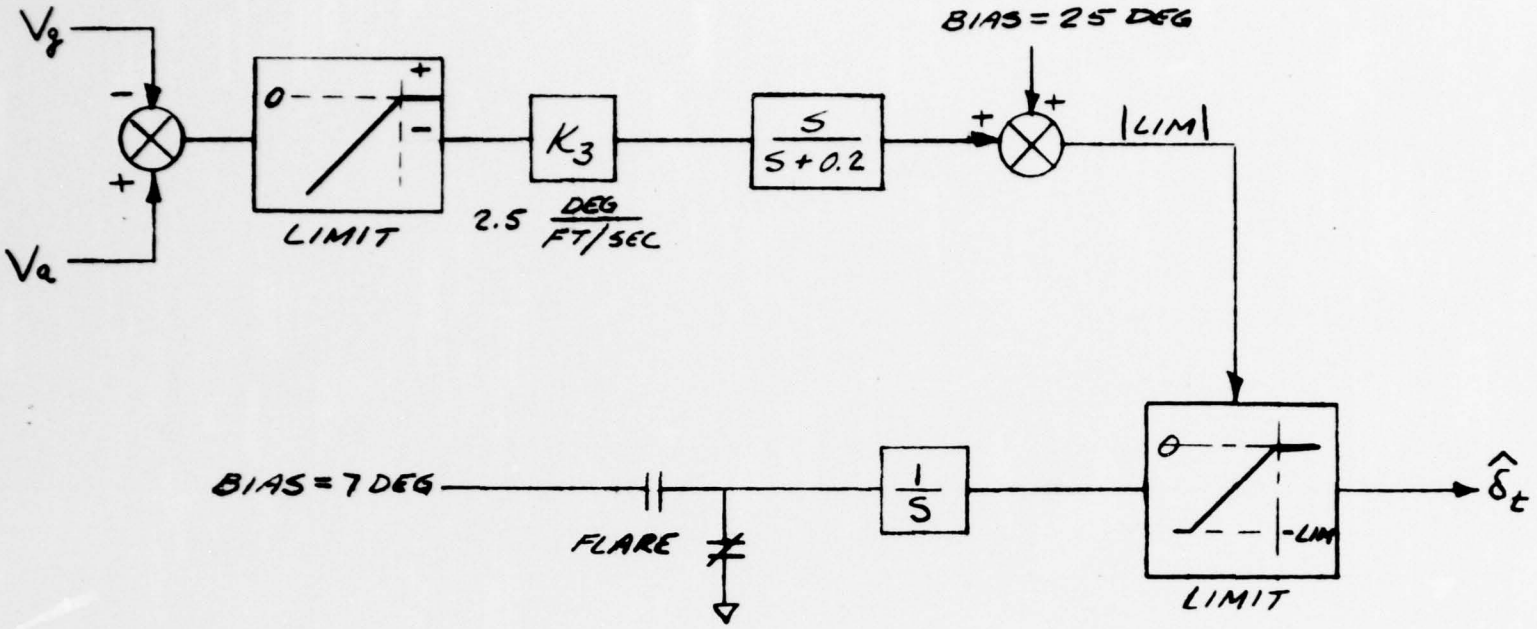

FIGURE 12. VARIABLE THROTTLE RETARD LIMIT CONFIGURATION #2

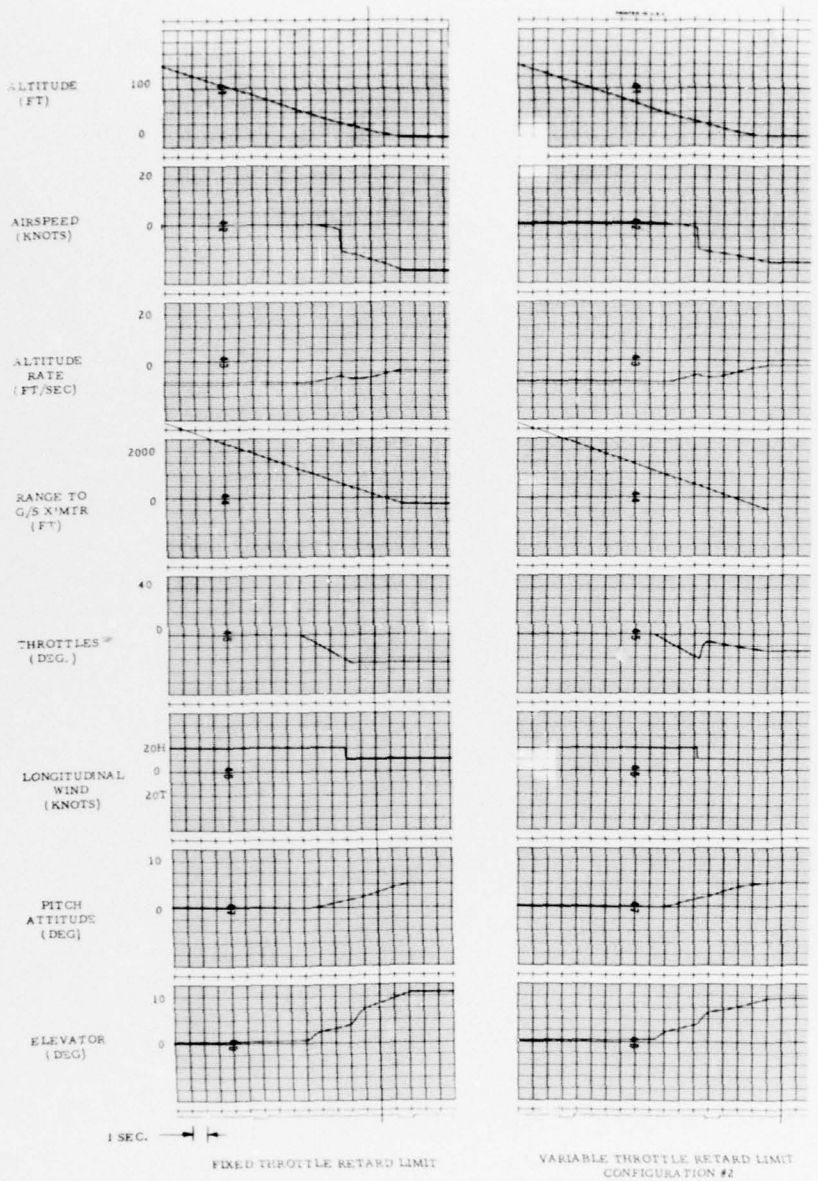

FIGURE 13. FLARE RESPONSES-KNIFE-EDGE SHEAR

SECTION 3

SIMULATION

The following perturbation equations were used to simulate the three degree of freedom longitudinal axis.

$$\ddot{\theta} = M_w w + M_{\dot{w}} \dot{w} + M_q \dot{\theta} + M_u u + M_{\delta T} \delta T + M_{\delta e} \delta e + M_H H + M_{\delta s} \delta s$$

$$\dot{w} = z_w w + z_{\dot{w}} \dot{w} + (V + z_q) \dot{\theta} + z_u u + z_{\delta e} \delta e + z_H H$$

$$\dot{u} = g\theta + x_w w + x_u u + x_{\delta T} \delta T + x_{\delta e} \delta e + x_H H$$

Parameters are defined in Figure 14.

The ground effect data obtained from Wright Field was as follows:

$$\Delta C_m = -0.138 \quad (1 - A/A_G)$$

$$\Delta C_L = +0.127 \quad (1 - A/A_G)$$

$$\Delta C_D = -0.045 \quad (1 - A/A_G)$$

where A_G is the effective aspect ratio in the presence of the ground. The quantity, $1-A/A_G$, designated by H, is shown in Figure 15, as a function of C.G. altitude.

The horizontal stabilizer, denoted above by δ_s, was simulated with a time rate of 0.15 degrees of surface per second. It was engaged whenever elevator deflection exceeded 1.5 degrees. The effectiveness of the stabilizer in producing a pitching moment was taken to be three times that of the elevator.

The twelve flight conditions at which existing aero data was derived are not representative of the gross weight to airspeed ratio that is currently being flown on approach. For this reason, a new flight condition was developed with a gross weight of 160,000 pounds and airspeed of 155 knots. Figure 14 shows the dimensional stability derivatives obtained from Wright Field for Flight Condition 2 defined with the same gross weight mentioned above, but an airspeed of 140 knots. The values for derivatives in the new flight condition were obtained by multiplying by the appropriate factor, 155/140 or $(155/140)^2$ as shown in Figure 14. For uniformity, this flight condition was simulated throughout the longitudinal study.

FIGURE 14. LONGITUDINAL DIMENSIONAL STABILITY DERIVATIVES

Parameter	Definition	Value at Flight Condition 2	Value this Flight Condition
M_w	$\frac{\rho s V \bar{c}}{2I_y} C_{m_\alpha}$	$-.6219 \times 10^{-2}$	$-.6916 \times 10^{-2}$
$M_{\dot{w}}$	$\frac{\rho s \bar{c}^2}{4I_y} C_{m_{\dot{\alpha}}}$	$-.1466 \times 10^{-2}$	$-.1466 \times 10^{-2}$
M_q	$\frac{\rho s V \bar{c}^2}{4I_y} C_{m_q}$	-.8554	-.9512
M_u	$\frac{\rho s V \bar{c}}{I_y} (C_m + C_{m_u})$	0	0
$M_{\delta T}$	$\frac{z_j}{I_y}$	$.1852 \times 10^{-5}$	$.1852 \times 10^{-5}$
$M_{\delta e}$	$\frac{\rho s V^2 \bar{c}}{2I_y} C_{m_{\delta e}}$	1.124	1.390
M_H	$\frac{\rho s V^2 \bar{c}}{2I_y} \Delta C_m$		-.2576
Z_w	$\frac{-\rho s V}{2m} (C_{L\alpha} + C_D)$	-.637	-.708
$Z_{\dot{w}}$	$\frac{-\rho s \bar{c}}{4m} C_{L\dot{\alpha}}$	-.0105	-.0105
Z_q	$\frac{-\rho s V \bar{c}}{4m} C_{Lq}$	-6.15	-6.84

Parameter	Definition	Value at Flight Condition 2	Value this Flight Condition
Z_u	$\frac{-\rho s V}{m}(C_L+C_{L_u})$	-.272	-.302
$Z_{\delta e}$	$\frac{-\rho s V^2}{2m} C_{L_{\delta e}}$	7.46	9.23
Z_H	$\frac{-\rho s V^2}{2m} \Delta C_L$		-5.113
X_w	$\frac{\rho s V}{2m}(C_L-C_{D\alpha})$	.0647	.0719
X_u	$\frac{-\rho s V}{m}(C_D+C_{D_u})$	-.0426	-.0474
$X_{\delta T}$	$\frac{1}{m}$	$.2013 \times 10^{-3}$	$.2013 \times 10^{-3}$
$X_{\delta e}$	$\frac{-\rho s V^2}{2m} C_{D_{\delta e}}$	1.49	1.84
X_H	$\frac{-\rho s V^2}{2m} \Delta C_D$		1.812
$M_{\delta s}$	$3 M_{\delta e}$	3.372	4.170

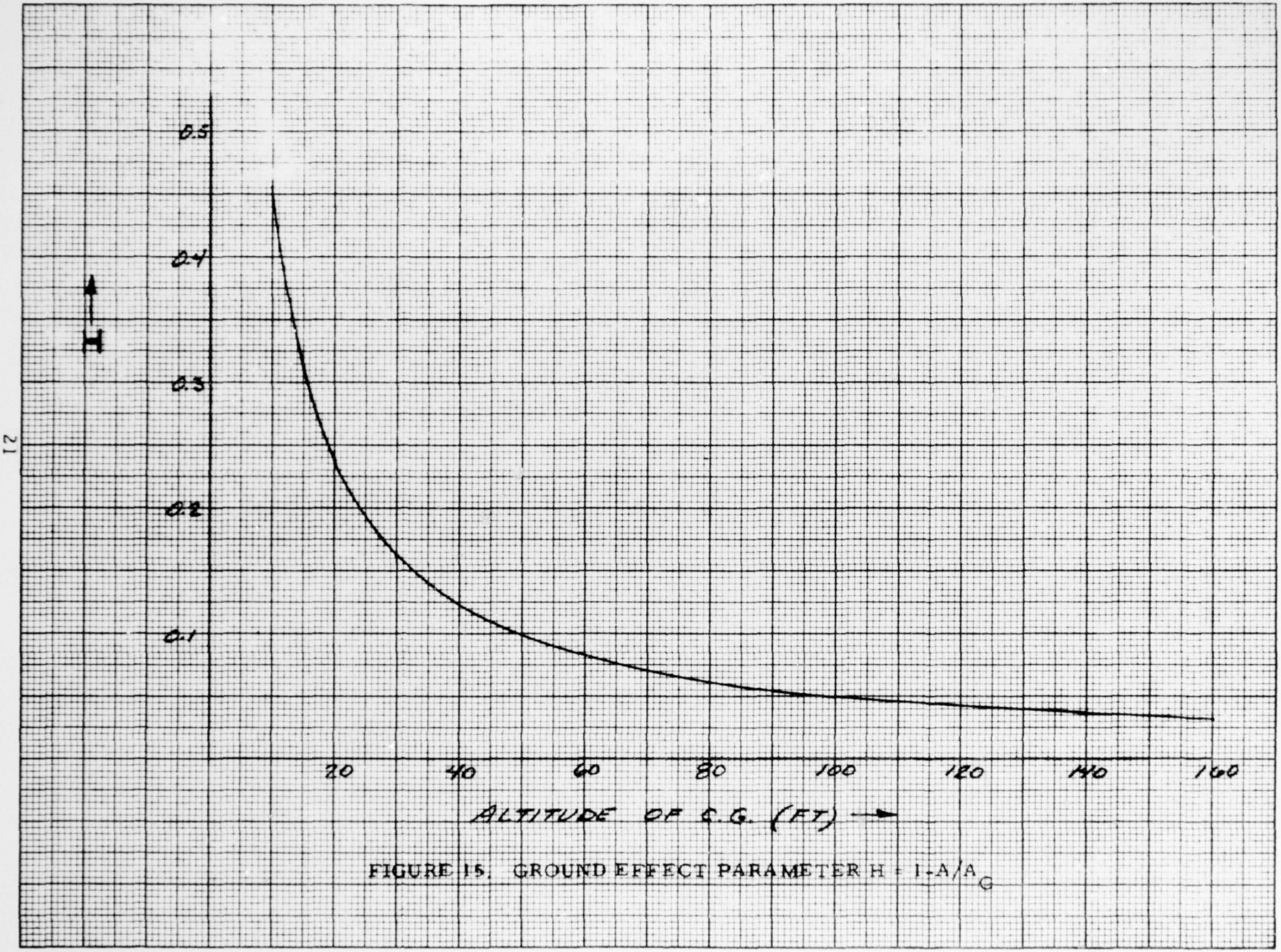

FIGURE 15. GROUND EFFECT PARAMETER $H = 1-A/A_G$

The characteristics of the logarithmic shears used in the above analyses are shown in Figure 16.

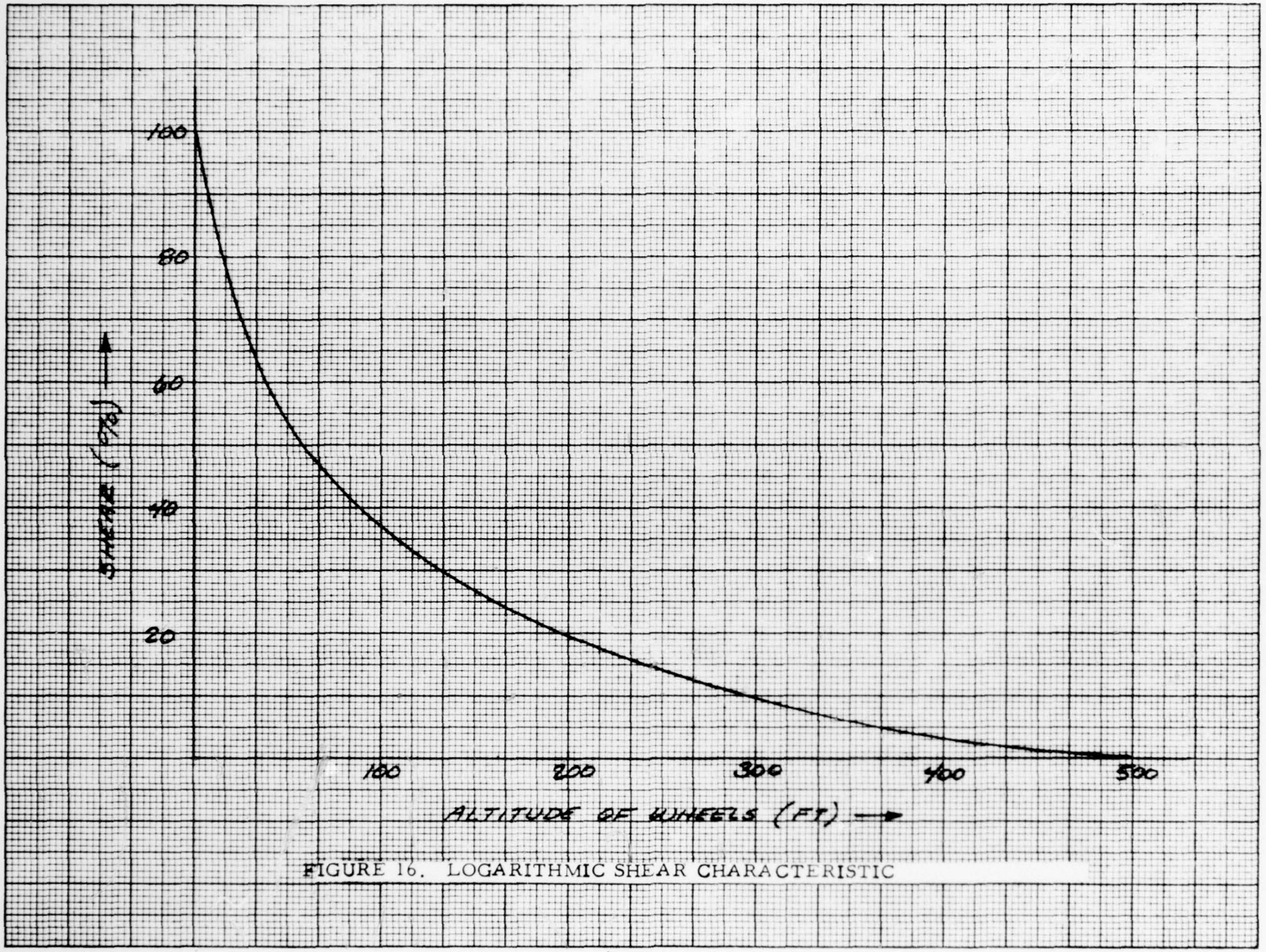

FIGURE 16. LOGARITHMIC SHEAR CHARACTERISTIC

SECTION 4

CONCLUSION

This study has investigated the feasibility of improving the flare performance, during automatic approach, through the use of inertial flight path angle (γ) and range. A comparison was made between it and the present system, which uses an exponential, altitude, altitude rate control law.

The proposed system which commands a γ, based upon altitude and range information, was found to yield improved performance under varying wind conditions. Longitudinal dispersions at touchdown were found to be much reduced in all cases with a slight improvement in overall touchdown sink rate variation.

A study was also performed in an effort to optimize the airspeed bleed during flare, for varying wind conditions, through the use of range rate information. Having investigated various forms of closed loop throttle retard systems, it was concluded that a non-linear system which varies the throttle retard limit as a function of ground speed and airspeed is the most promising. However, it must not affect throttles on a long term basis since flare performance would then become a function of winds due to pitching moment due to thrust ($M_{\Delta T}$). Therefore, a system adjusting retard limit on a short term basis, to compensate airspeed during extreme shears, is proposed. Such a configuration has been shown to yield significant improvements during knife-edge shears.

APPENDIX

The altitude command ($\hat{h}$) function of range (R) was established to fix in space a path similar to that of the nominal exponential flare, in the presence of zero winds. The function was derived as follows;

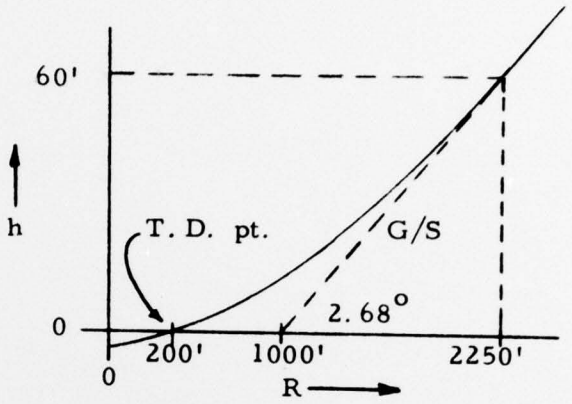

Let;

$$h = aR^2 + bR + c;$$

$$\therefore \frac{dh}{dR} = 2a\,R + b$$

Constraints; at $h = 60'$, $R = 2250'$; $\frac{dh}{dr} = \frac{2.68°}{57.3} = .0467$ (rad)

at $h = 0'$, $R = 200'$; $\frac{dh}{dr} = 0.5$ (deg.) $= .0087$ (rad)

(1) $0 = a(200)^2 + b(200) + c$

(2) $2a(2250') + b = .0467$

(3) $2a(200') + b = .0087$

subtracting (3) from (2);

$$2a\,(2050) = .0467 - .0087 = .0380$$

$$\therefore a = 9.3 \times 10^{-6}$$

$$b = .0062$$

from equation (1);

$$c = -1.6$$

$$\therefore \text{use} \quad \boxed{\hat{h} = 9.3 \left(\frac{R}{1000}\right)^2 + 6.2 \left(\frac{R}{1000}\right) - 1.6}$$

This function has been plotted in Figure 17.

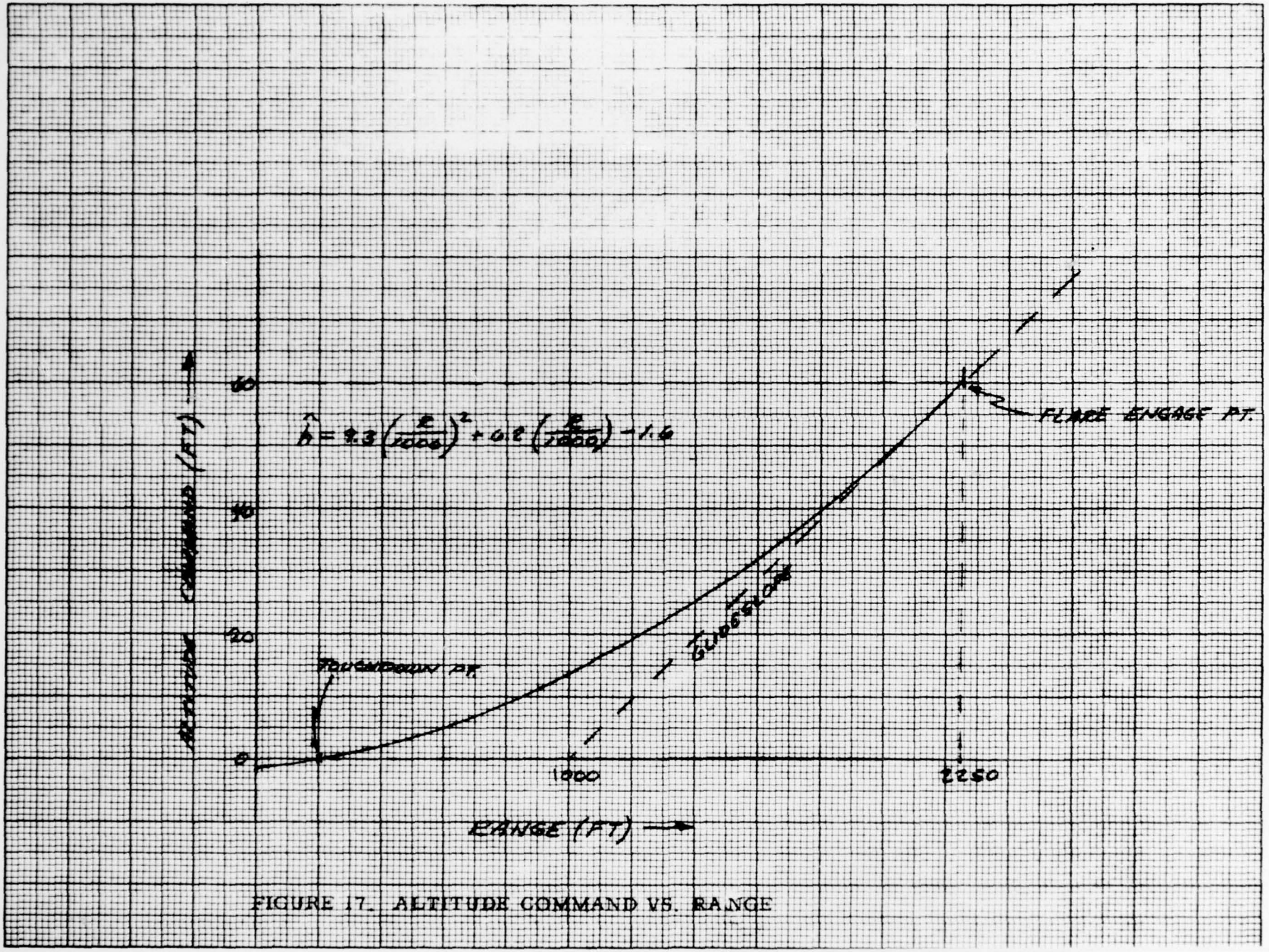

FIGURE 17. ALTITUDE COMMAND VS. RANGE